

# Thermal Transport as a Probe of Localized Charge and Lattice Distortions in Manganites and Cuprates

J. L. Cohn

Department of Physics, University of Miami, Coral Gables, FL 33124

The thermal resistivity of manganites and cuprates is shown to correlate with local lattice distortions and the presence of localized holes as determined from neutron diffraction and nuclear quadrupole resonance. Oxygen doping dependent studies of heat conduction in Y-123 and Hg cuprates suggest that a fraction of the holes in the  $\text{CuO}_2$  planes are localized near the planar hole concentration  $p = 1/8$ . The results are consistent with the formation of short-ranged, static stripe domains that are pinned near oxygen vacancy clusters.

PACS numbers: 74.72.-h, 74.25.Fy, 74.25.Bt, 74.25.Dw

Manganite perovskites and cuprate superconductors are both typified by local lattice distortions. In the colossal magnetoresistance manganites correlations of the local structure with charge transport through the insulator-metal transition demonstrate that the distortions are associated with localized holes (polarons).<sup>1,2</sup> In the cuprates the distortions are smaller in magnitude and are not as obviously related to the localization of doped holes. Nuclear magnetic and quadrupole resonance (NMR and NQR) studies<sup>3,4</sup> of  $\text{La}_{1-x}\text{Sr}_x\text{CuO}_4$  (La-214) and  $\text{YBa}_2\text{Cu}_3\text{O}_{6+x}$  (Y-123) indicate the presence of localized holes in the  $\text{CuO}_2$  planes. Whether localized holes are a general feature of cuprates, organize in charge/spin stripes,<sup>5</sup> or contribute to the normal-state pseudogap<sup>6,7</sup> are fundamental issues of current interest.

Here we demonstrate that the thermal resistivity of manganites and in the normal state of cuprates is a sensitive measure of lattice distortions. For the cuprates the change in slope of the thermal conductivity ( $\kappa$ ) at  $T_c$  is also shown to be a measure of the difference between the normal- and superconducting-state low-energy electronic spectral weight (proportional to the superfluid density). The phase behavior of these two thermal transport parameters for  $\text{YBa}_2\text{Cu}_3\text{O}_{6+x}$  (Y-123) and Hg cuprates reveal anomalies near planar hole concentrations  $p = 1/8$  which are attributed to localized holes in the  $\text{CuO}_2$  planes. The implications are discussed.

The thermal resistivity<sup>8</sup> of undoped  $\text{LaMnO}_3$  is surprisingly high for a crystalline insulator ( $\sim 1\text{mK/W}$ ), approaching the theoretical maximum value<sup>9</sup> and indicative of a high degree of disorder. Such behavior in crystalline materials is characteristic of random, noncentral distortions of the lattice, attributable in the manganites to Jahn-Teller distortions of the  $\text{MnO}_6$  octahedra. Figure 1 shows that the lattice thermal resistivity,  $W_L = \kappa_L^{-1}$ , of doped compounds correlates with a measure of the bond disorder determined from neutron diffraction,  $D \equiv (1/3) \sum_{i=1}^3 |(u_i - \bar{u})/\bar{u}| \times 100$ , with  $u_i$  the Mn-O bond lengths, and  $\bar{u} = (u_1 u_2 u_3)^{1/3}$ . The correlation is especially convincing given that  $D$  is dramatically altered by the ferromagnetic and charge-ordering transitions upon cooling from the paramagnetic insulating

state (Fig. 1, inset). For example,  $\text{Pr}_{0.5}\text{Sr}_{0.5}\text{MnO}_3$  has the smallest  $D$  at 300K, but one of the largest at 35K; the reverse is true for  $\text{La}_{0.7}\text{Ca}_{0.3}\text{MnO}_3$ . The various phase transitions all involve modifications of the local structure which correlate with hole itinerancy and the magnetism, confirming their polaronic origin.

We have conducted extensive studies of  $\kappa$  vs temperature and oxygen doping in polycrystalline and single-crystal (ab-plane) Y-123 and Hg cuprates.<sup>10,11</sup> Figure 2 (a) shows, for Y-123 crystals and polycrystals at  $T=100\text{K}$ , the doping dependence of the thermal resistivities, expressed as relative changes from values at optimum doping ( $p=0.16$ ). The hole concentration per planar Cu atom,  $p$ , was determined from thermopower measurements and the empirical relations with bond va-

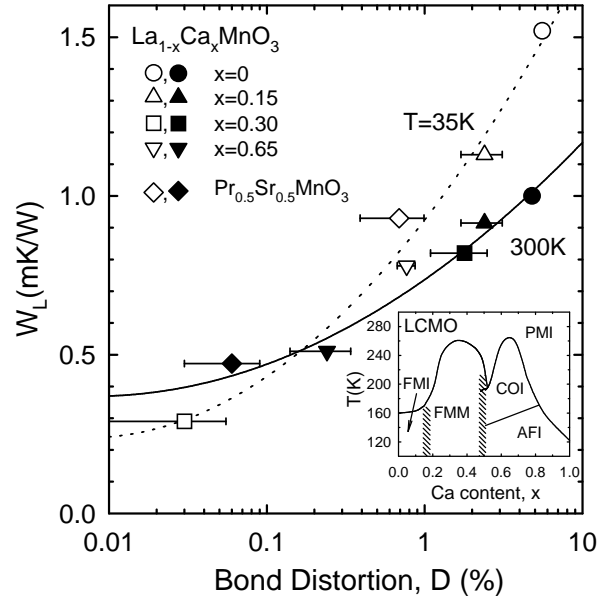


FIG. 1. Lattice thermal resistivity vs Mn-O bond distortion (see text) for manganite polycrystals (Ref. 8). The phase diagram for  $\text{La}_{1-x}\text{Ca}_x\text{MnO}_3$  is shown in the inset, delineating the paramagnetic insulating (PMI), ferromagnetic insulating (FMI), ferromagnetic metallic (FMM), charge-ordered insulating (COI), and antiferromagnetic insulating (AFI) regimes.

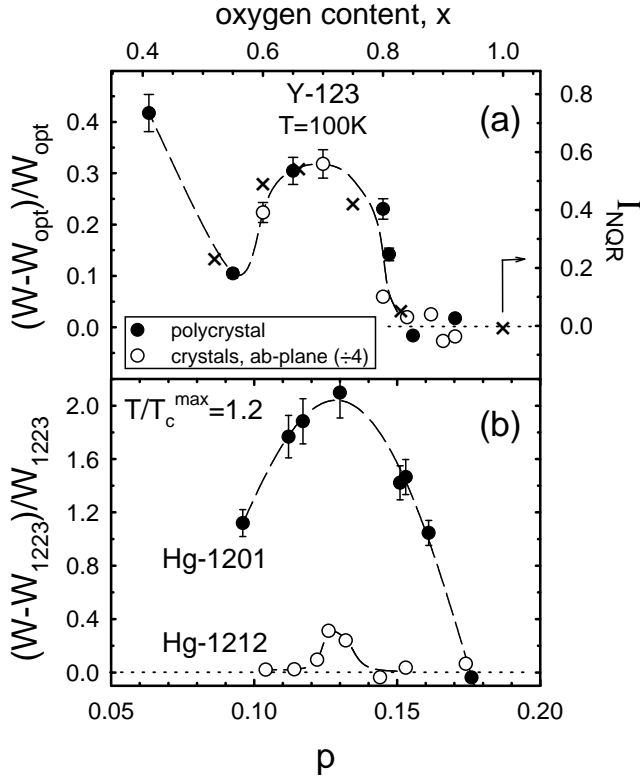


FIG. 2. (a) Thermal resistivity at  $T=100\text{K}$  relative to that at  $p_{opt} = 0.16$  for Y-123 polycrystals and the ab-plane of single crystals (Ref. 10) [ $W_{opt} = 0.21\text{mK/W}$  (0.08mK/W) for the polycrystal (crystals)]. Also plotted ( $\times$ 's) is the relative intensity of anomalous  $^{63}\text{Cu}$  NQR signals (Ref. 4). The dashed curve is a guide to the eye. (b) Thermal resistivity for Hg-1201 and Hg-1212 polycrystals relative to that of Hg-1223 (Ref. 11). Dashed curves are guides.

lence sums established by Tallon *et al.*<sup>12</sup> In spite of additional thermal resistance due to  $c$ -axis heat flow and granularity in the polycrystal, the doping dependence is essentially the same as that of the ab-plane of crystals. The behavior thus reflects the intrinsic oxygen doping dependence of the thermal resistivity for heat flow in the planes.

Given that the electronic thermal conductivity ( $\kappa_e$ ) at  $T > T_c$  in optimally doped, single-crystal Y-123 represents only  $\sim 10\%$  of the total  $\kappa = \kappa_e + \kappa_L$ ,<sup>13</sup> the data imply a lattice thermal resistivity that is anomalously enhanced about  $p = 1/8$ . This enhancement correlates quite well with the relative intensity [ $I_{NQR}$ , Fig. 2 (a)] of anomalous  $^{63}\text{Cu}$  NQR signals from planar Cu (below 30.8MHz), attributed to localized holes in the planes.<sup>4</sup>

Similarly enhanced thermal resistivities about  $p=1/8$  are observed in studies<sup>11</sup> of  $\text{HgBa}_2\text{Ca}_{m-1}\text{Cu}_m\text{O}_{2m+2+\delta}$  [Hg-1201 ( $m=1$ ), Hg-1212 ( $m=2$ ), Hg-1223 ( $m=3$ )]. As we discuss further below, Hg-1223 shows no apparent anomaly, so we use its  $W(p)$  curve as a reference to plot the relative thermal resistivities of the other compounds in Fig. 2 (b). These data provide some insight into the role of oxygen vacancies in this phenomenon. A single

$\text{HgO}_\delta$  layer per unit cell contributes charge to  $m$  planes in  $\text{Hg-12}(m-1)m$  so that the oxygen occupancy  $\delta$  increases with  $m$ . At optimum doping,<sup>14</sup>  $\delta_{opt} \simeq 0.18$  (Hg-1201), 0.35 (Hg-1212) and 0.41 (Hg-1223). The anomalous thermal resistivity and the range in  $p$  over which it occurs increase with the vacancy concentration,  $1 - \delta$ .

A further indication that the lattice distortions responsible for enhanced thermal resistivity are associated with localized holes comes from the behavior of the slope change in  $\kappa$  at  $T_c$ . Figure 3 shows the phase behavior of the dimensionless superconducting-state slope change<sup>10</sup> defined as  $\Gamma \equiv -d(\kappa^s/\kappa^n)/dt|_{t=1}$ , where  $t = T/T_c$  and  $\kappa^s(\kappa^n)$  is the thermal conductivity in the superconducting (normal) state.  $\Gamma$  measures the change in scattering of heat carriers (electrons and phonons) induced by superconductivity. Particularly striking is the similarity between the electronic specific heat jump for Y-123,<sup>6</sup>  $\Delta\gamma/\gamma(p)$ , and  $\Gamma(p)$ ; both quantities exhibit minima near  $p = 1/8$ .

Though the origin of the slope change in  $\kappa$  at  $T_c$  (i.e. electronic or phononic) has been a subject of some debate, the results of Fig. 3 (a) demonstrate unambiguously that  $\Gamma$ , like  $\Delta\gamma/\gamma$ , measures the difference between

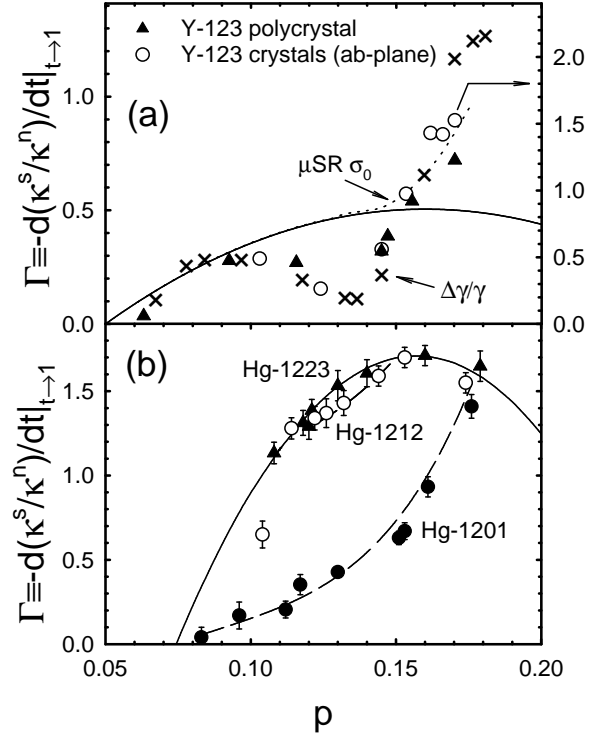


FIG. 3. (a) The normalized slope change in  $\kappa(T)$  at  $T_c$  vs doping for each of the Y-123 specimens from Fig. 2 (a). Also shown are the normalized electronic specific heat jump,  $\Delta\gamma/\gamma$ , from Loram *et al.* (Ref. 6) ( $\times$ 's), and the  $\mu\text{SR}$  depolarization rate from Ref. 15 (dotted curve), divided by 1.4 and 2.7, respectively, and referred to the right ordinate. The solid line is  $0.51 - 41.7(p - 0.16)^2$ . (b) The normalized slope change in  $\kappa(T)$  at  $T_c$  vs doping for Hg cuprates. The solid line is  $1.71 - 250(p - 0.157)^2$ . Dashed curves are guides.

the normal- and superconducting-state low-energy electronic spectral weight. The muon spin rotation ( $\mu$ SR) depolarization rate ( $\sigma_0$ ),<sup>15</sup> a measure of the superfluid density, matches the data for  $\Gamma$  and  $\Delta\gamma/\gamma$  at  $p < 0.09$  and  $p > 0.15$  when suitably scaled [dotted curve in Fig. 3 (a)]. The sharp rise in  $\sigma_0$  for  $p > 0.15$  is due to the superconducting condensate on oxygen-filled chains,<sup>15</sup> motivating the solid curve in Fig. 3 (a)] as an estimate of  $\Gamma(p)$  for the  $\text{CuO}_2$  planes alone in Y-123. The range of  $p$  over which  $\Gamma$  and  $\Delta\gamma/\gamma$  deviate from the  $\mu$ SR curve *coincides* with the range of enhanced thermal resistivity. The suppressed transfer of spectral weight below  $T_c$  is also consistent with the localization of a fraction of planar holes. That  $\sigma_0$  is not also suppressed near  $p=1/8$  indicates that hole-localized domains do not inhibit the formation of a flux lattice in adjacent regions where holes are itinerant.

The  $\Gamma(p)$  data for the Hg cuprates [Fig. 3 (b)] tell a similar story. For Hg-1223  $\Gamma(p)$  describes an inverted parabola centered near  $p = 0.16$  (solid curve), with the data for Hg-1212 and Hg-1201 suppressed from this curve in ranges of  $p$  that coincide with those where  $W(p)$  is enhanced. Evidently the concentration of localized holes in Hg-1223 is sufficiently small that neither  $\Gamma$  nor  $W$  exhibit anomalies.

If our interpretation about localized holes is correct, the Hg data make it clear that oxygen vacancies play only a supporting role. The importance of 1/8th doping implies that the phenomenon involves an excitation of the  $\text{CuO}_2$  planes that is commensurate with the lattice. A plausible candidate is a small domain of static stripe order,<sup>5</sup> nucleated via pinning by a vacancy-induced mechanism. Recent Raman scattering studies of optimally-doped Hg compounds<sup>16</sup> implicate vacancy clusters in pinning: the oscillator strength of the  $590\text{ cm}^{-1}$  mode, attributed to c-axis vibrations of apical oxygen in an environment of four vacant nearest-neighbor dopant sites, scales with the magnitudes of the  $W$  enhancement and  $\Gamma$  suppression. Oxygen vacancies in both Y-123 and Hg cuprates<sup>14,17</sup> displace neighboring  $\text{Ba}^{2+}$  toward the  $\text{CuO}_2$  planes. The bonding of Ba with apical oxygen could lead to local distortions of the  $\text{CuO}$  polyhedra that pin a charge stripe. Alternatively, a magnetic mechanism is possible. In the Hg cuprates the shift of Ba atoms associated with a cluster of four vacancies nearest a  $\text{CuO}$  polyhedron will induce a positive potential in the planes that inhibits its occupation by a hole, thereby suppressing spin fluctuations and possibly fixing a  $\text{Cu}^{2+}$  spin at the site. Larger vacancy clusters, surrounding adjacent  $\text{CuO}$  polyhedra oriented along  $\langle 100 \rangle$  directions, may induce several spins to order antiferromagnetically via superexchange. The presence of this spin-chain fragment would favor charge/spin segregation that is characteristic of stripe order.

Consider the relevant length scales. If randomly distributed, static stripe domains are to scatter phonons, their in-plane extent must be less than the phonon mean-free-path,  $\Lambda$ , and their mean separation comparable to  $\Lambda$ .

Expressing  $\Lambda^{-1}$  as a sum of terms for scattering by these domains and by all other processes,  $\Lambda^{-1} = \Lambda_{\text{str}}^{-1} + \Lambda_{\text{other}}^{-1}$ , we use the in-plane thermal resistivity for Y-123 and kinetic theory to find<sup>18</sup>  $\Lambda_{\text{str}} \simeq [3/C_L v \Delta W(p=1/8)] \simeq 70\text{\AA}$  as an estimate of the separation between domains at  $p=1/8$ . We can make a rough estimate of the fractional area of the planes having static stripes by taking the typical domain size to be  $2a \times 8a$  ( $a$  is the lattice constant), the stripe unit cell suggested<sup>5</sup> for (La,Nd)-214. This yields a fraction  $16(a/\Lambda_{\text{str}})^2 \simeq 0.05$ . Our data suggest that this fraction is substantially higher in Hg-1201, but apparently below the 2-D percolation threshold of 0.50. This presumably explains why no substantial  $T_c$  suppression is observed near  $p=1/8$  in Y-123 or the Hg cuprates, in contrast to the case of (La,Nd)-124; stripe domains in the latter system have longer-range order ( $\geq 170\text{\AA}$ ).<sup>5</sup>

This work was supported by NSF Grant No. DMR-9631236.

- 
- <sup>1</sup> P. G. Radaelli *et al.*, Phys. Rev. B **54**, 8992 (1996); C. H. Booth *et al.*, *ibid.*, R15606 (1996); D. Louca *et al.*, *ibid.* **56**, R8475 (1997).
  - <sup>2</sup> C. H. Booth *et al.*, Phys. Rev. Lett. **80**, 853 (1998).
  - <sup>3</sup> P. C. Hammel *et al.*, Phys. Rev. B **57**, R712 (1998).
  - <sup>4</sup> P. C. Hammel and D. J. Scalapino, Phil. Mag. **74**, 523 (1996); H. Yasuoka *et al.*, Phase Trans. **15**, 183 (1989).
  - <sup>5</sup> J. M. Tranquada *et al.*, Nature **375**, 561 (1995); Phys. Rev. B **54**, 7489 (1996); Phys. Rev. Lett. **78**, 338 (1997); cond-mat/9702117; cond-mat/9709325.
  - <sup>6</sup> J. W. Loram *et al.*, Phys. Rev. Lett. **73**, 1721 (1993); J. W. Loram *et al.*, J. Supercond. **7**, 243 (1994).
  - <sup>7</sup> B. Battlogg *et al.*, Physica C **235-240**, 130 (1994); B. N. Basov *et al.*, Phys. Rev. B **50**, 3511 (1994); J. L. Tallon *et al.*, Phys. Rev. Lett. **75**, 4414 (1995); A. Loeser *et al.*, Science **273**, 325 (1996); G. V. M. Williams *et al.*, Phys. Rev. Lett. **78**, 721 (1997).
  - <sup>8</sup> J. L. Cohn *et al.*, Phys. Rev. B **56**, R8495 (1997).
  - <sup>9</sup> D. G. Cahill, S. K. Watson, and R. O. Pohl, Phys. Rev. B **46**, 6131 (1992).
  - <sup>10</sup> C. P. Popoviciu and J. L. Cohn, Phys. Rev. B **55**, 3155 (1997); J. L. Cohn, *ibid.* **53**, R2963 (1996).
  - <sup>11</sup> J. L. Cohn *et al.*, unpublished.
  - <sup>12</sup> J. L. Tallon *et al.*, Phys. Rev. B **51**, 12911 (1995).
  - <sup>13</sup> K. Krishana *et al.*, Phys. Rev. Lett. **75**, 3529 (1995).
  - <sup>14</sup> O. Chmaissem *et al.*, Physica C **217**, 265 (1993); E. V. Antipov *et al.*, *ibid.* **218**, 348 (1993); Q. Huang *et al.*, Phys. Rev. B **52**, 462 (1995).
  - <sup>15</sup> Y. J. Uemura *et al.*, Phys. Rev. Lett. **66**, 2665 (1991); J. L. Tallon *et al.*, *ibid.* **74**, 1008 (1995).
  - <sup>16</sup> X. Zhou *et al.*, Phys. Rev. B **54**, 6137 (1996).
  - <sup>17</sup> J. D. Jorgensen *et al.*, Phys. Rev. B **41**, 1863 (1990).
  - <sup>18</sup> We take  $C_L(100\text{K})=1.3 \times 10^6\text{ J/m}^3\text{K}$  (Ref. 6) and  $v = 3 \times 10^3\text{ m/s}$  estimated from dispersion curves [L. Pintschovius *et al.*, Physica C **185-189**, 156 (1991)].